Int J Adv Manuf Technol (2015) 81:1023–1032
DOI 10.1007/s00170-015-7278-9

ORIGINAL ARTICLE

Energy criteria for machining-induced residual stresses in face milling and their relation with cutting power

Yuan Ma[1] · **Pingfa Feng**[1] · **Jianfu Zhang**[1] · **Zhijun Wu**[1] · **Dingwen Yu**[1]

Received: 4 January 2015 / Accepted: 4 May 2015 / Published online: 16 May 2015

Abstract Machining-induced residual stresses can significantly influence the performance of machined parts, and many scholars have contributed efforts to measure, evaluate, predict, and control the distribution of residual stresses. In most published researches, the residual stresses are analyzed as the function of cutting parameters, tool parameters, or material properties, but any of these parameters cannot decide the distribution of residual stresses solo and directly. And the commonly used evaluation criteria, like surface value, peak value, and existing range, cannot reflect the overall distribution of residual stresses. In this paper, a new approach to study this issue was proposed, and the cutting loads, the cutting parameters, and the evaluation of residual stress field were unified to the concept of energy and its mutual transformation with mechanical work. The effective cutting power on the machined surface was analyzed, and the integral of strain energy density over depth and the power of stored strain energy were supposed to be the energy criteria of residual stress field. Face milling experiments were carried out, and the cutting forces and the in-depth residual stress distribution were measured. According to the methodology proposed, the results showed that with the increase of effective cutting power, the power of stored strain energy increases with growing rate, which means that the partition of cutting work stored as strain energy increases simultaneously. And the integral of strain energy density over depth grows linearly with the effective cutting power under the experimental conditions in this study.

✉ Pingfa Feng
fengpf@tsinghua.edu.cn

[1] State Key Laboratory of Tribology, Department of Mechanical Engineering, Tsinghua University, Beijing 100084, China

Keywords Residual stress · Stored strain energy · Cutting power · Cutting force · Face milling

1 Introduction

Residual stresses in surface and subsurface layer of a machined component significantly influence the fatigue life, corrosion resistance, and abrasive resistance of the parts [1–3]. And residual stresses are also a major cause of machining distortion and dimensional instability for thin-walled structures [4]. Machining is the last manufacturing procedure for many industrial products; thus, it is very important to accurately predict and effectively control the machining-induced residual stresses.

For the past several decades, many researches have been carried out on machining-induced residual stresses. In most studies, residual stresses are regarded as the function of cutting parameters, tool parameters, or the properties of the workpiece material [5]. In these studies, a group of parameters are chosen, and after machining experiments, the value of surface residual stress or the pattern of stress distribution are measured and analyzed. In some researches, scholars proposed prediction models in different forms, mostly based on data fitting technology. El-Khabeery and Fattouh [6] studied the influence of cutting speed, feed rate, and depth of cut on the value of surface residual stress, and a second-order polynomial empirical model was proposed to predict the surface stress. The study of El-Axir [7] covered the influence of cutting speed, feed rate, and the tensile strength of material, and a complicated polynomial empirical model to predict the stress distribution after machining was proposed. Capello [8, 9] carried out a comprehensive study on the relation between machining conditions and surface residual stress, taking into account the influence of cutting parameters, the tool geometry parameters,

and the chemical composition of workpiece material, and the prediction model proposed specifies the variant effect of each parameter. He et al. [10] used exponential model, which is widely used in predicting cutting forces, to specify the influence of different cutting parameters and pre-stress on machining-induced residual stresses. Intelligent algorithms have also been introduced. Jafarian et al. [11] established an intelligent system with artificial neural network and genetic algorithm to improve surface integrity considering parameters like residual stresses and roughness. A great many similar studies with various design variables on different materials and different machining processes have been published, and the conclusions are helpful to understand the formation mechanism and distribution law of machining-induced residual stresses from different aspects. But as stated by Outeiro et al. [5], it is difficult to achieve a unified conclusion on the influence of a single parameter under the commonly used criteria evaluating the machining-induced residual stresses, like the value of surface residual stress, the peak value of the tensile/compressive stress, the influencing range of machining-induced residual stresses, and the depth of the peak value.

Here, it might as well take the influence of cutting speed as an example, which is among the most frequently studied in this issue. In the research of M'Saoubi et al. [12] and Arunachalam et al. [13], the surface residual stresses tend to be more tensile with growing cutting speed, while the experiments done by Outeiro et al. [5] and the finite element analysis of Zong et al. [14] showed an opposite trend. And in Capello's prediction model [8], the influence of cutting speed is not considered as this influence is not significant according to their former research. In analyzing the influence of many other parameters, similar inconformity can be found. The differences in experimental conditions and ranges of parameters might be the main reason leading to the different conclusions, or maybe, it is needed to look into this issue from other perspectives. One early research done by El-Khabeery and Fattouh [6], with not so advanced measuring technology, indicated the coupled influence of different parameter pairs. This might not be enough. All the cutting parameters, tool parameters, material properties, and maybe some other conditions work synergistically to decide the distribution of residual stresses.

It is widely accepted that the non-uniform plastic deformation caused by mechanical or thermal loads and changes of phase or density are the main sources of residual stresses [3, 15]. In normal machining process, the temperature is controlled much lower than the phase changing temperature of the workpiece material, and thus the coupling thermomechanical loads are often used as the main sources of machining-induced residual stresses in the theoretical analysis [16, 17]. Yao et al. [18] analyzed the formation mechanism of machining-induced residual stresses in detail and specified the effects of cutting forces and temperature. Ma et al. [19] analyzed the evolution mechanism of the stress field during machining process with finite element method, illustrating the three stress zones in front of the cutting edge, along the reverse extension direction of the shear deformation zone and near the machined surface due to the cutting forces and temperature gradient. As cutting forces are much easier to measure than stress and temperature distribution, it is of practical significance if the stress distribution can be predicted with measured cutting forces. But as a matter of fact, most experimental studies on residual stresses did not include the measurement of cutting forces, and most of those that measured cutting forces just considered them as the function of cutting parameters and a reference for analyzing the measured results of residual stresses [12, 20–22], while little direct and quantitative analysis of the relation between cutting forces and stress distribution is carried out. Outeiro et al. [5] evaluated the surface residual stresses in function of the three orthogonal components of cutting force and the temperature, which might be a new clue to understand residual stresses. Unfortunately, no obvious trend was found, and Outeiro et al. concluded that cutting forces seem to be of small help to predict residual stresses if being taken alone.

Following the analysis given above, there are two problems need to be solved. Firstly, new physical quantities or concepts that can connect forces, stresses, and temperature are needed for the theoretical analysis on the formation mechanism of residual stresses. Secondly, the commonly used criteria of residual stresses can only reflect limited aspects of residual stress distribution, leaving the overall state of stress field unrevealed, and new criteria are needed to fill this gap. The solution of these two problems may come to the same exit, the concept of energy, the work, and their reciprocal transformation.

In this study, the power of work done to the workpiece and its effective partition on the machined surface are analyzed and calculated, which can be analyzed as the function of cutting forces, speeds, and the cutting edge radius of the tool. A large partition of work done to the workpiece may dissipate as heat and result in the large-gradient temperature field. And another partition of the cutting work is stored in the workpiece material. The residual stress field is supposed to be the outward manifestation of the stored energy. The integral of strain energy density over depth and the power of stored strain energy are proposed to be the energy criteria of machining-induced residual stresses. A group of experiments were performed, and the cutting forces and the in-depth distribution of residual stresses were measured. The cutting power items were analyzed, and the residual stress distribution of each test was evaluated with the proposed energy criteria.

2 Theoretical analysis

2.1 Effective cutting power in face milling

Power is the rate of mechanical work, and cutting power is often calculated with the cutting parameters and the corresponding cutting force components that can be measured with a multi-channel dynamometer or be predicted with empirical or theoretical models [23, 24]. Shao et al. [25] proposed a simplified prediction model for cutting power, where the tangential component of the cutting force, as well as the corresponding cutting power, is divided into two parts and estimated with empirical models, respectively. Though the sources of the power consumption were not specified clearly in this research, the prediction model infers that the total cutting power can be divided into the power needed to remove certain volume of workpiece material (termed as chip formation power in this paper) and the power consumed due to the frictional movement between tool and workpiece (termed as frictional power in this paper).

It is not difficult to achieve a real-time measurement of three-directional cutting forces with currently available techniques, and in this study, we proposed a method to calculate cutting power with the measured cutting forces. A simplified three-dimensional calculation diagram of cutting forces and speeds is shown as Fig. 1, where F_x, F_y, and F_z are the total cutting forces along feeding (x), peripheral (y), and axial (z) directions, respectively, which can be measured directly with a three-directional dynamometer; F_F is the frictional force between the machined surface and the relief face of the tool, and F_{Fx} and F_{Fy} are the components of F_F along x and y directions, respectively; F_{Cx} and F_{Cy} are chip formation forces in xOy plane; v_x and v_y are the speeds of the engaged tool tip along feed and peripheral directions, respectively, and v_r is the resultant velocity in xOy plane; φ is the angle between v_r and v_x. It is worthy of notice that the frictional movement between formed chip and the rake face of the cutting tool may also contribute to the three-directional cutting forces, but as it is difficult to accurately predict the chip flow velocity and direction in milling, in this study, this component was not specified in the calculation of cutting power. The frictional force in Fig. 1 is assumed to be just acting on the machined surface and can be calculated directly with the measured axial cutting force.

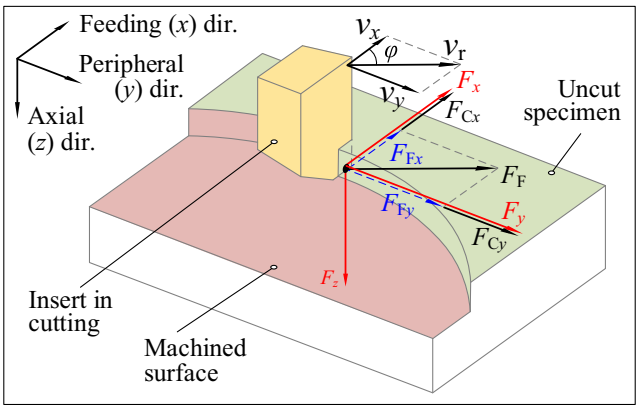

Fig. 1 Simplified model for the cutting forces and velocities in face milling

Based on the analysis above, the components of cutting power can be calculated with Eq. (1).

$$\begin{aligned} &P_T = P_F + P_C \\ &P_F = F_F v_r \\ &P_C = F_{Cx} v_x + F_{Cy} v_y = (F_x - F_{Fx}) v_x + (F_y - F_{Fy}) v_y \\ &F_F = \mu F_z\ ,\quad v_r = \sqrt{v_x^2 + v_y^2} \\ &F_{Fx} = F_F \cdot \cos\varphi\ ,\quad F_{Fy} = F_F \cdot \sin\varphi\ ,\quad \varphi = \arctan(v_y / v_x) \end{aligned} \tag{1}$$

where P_T is the total cutting power; P_F is the frictional power; P_C is the chip formation power; μ is the friction coefficient between tool and workpiece material under cutting conditions.

It is worthy of notice that not all the cutting power is done to the machined surface. The work done by F_{Cx} and F_{Cy} are mostly on the chip and is taken away continuously during machining process; however, due to the rounded cutting edge, part of the material in front of the cutting edge may flow downwards and become part of the machined surface, and a separation point exists ahead of the stagnation zone [26–28], as shown in Fig. 2. The experimental research carried out by Ozturk and Altan [27] showed that the height of separation point from the nominal machined surface (a) is a variable decided by the cutting conditions like tool edge radius (r_ε), depth of cut (t), cutting speed (v), and the value of the separation angle (ξ) lies between 56° and 64° under the conditions of their experiment. Much experimental and theoretical research still needs to be done to model the material behavior during machining process and to predict the accurate position of the separation point. For the time being and as an approximation, the separation angle can be assumed to be a constant, $\xi \equiv 60°$, and the height of the separation point from the nominal machined surface (a) is approximately equal to one half of the edge radius, $a \approx (1 - \cos\xi)\, r_\varepsilon = 0.5 r_\varepsilon$.

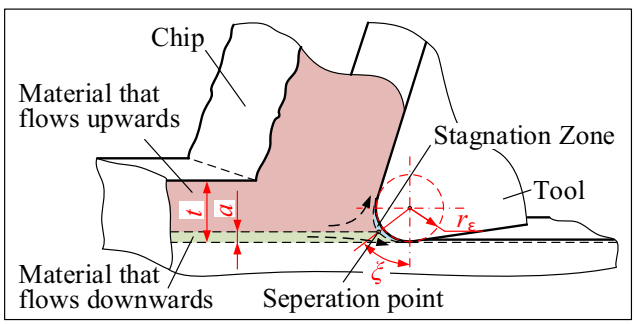

Fig. 2 Schematic of material flow with rounded cutting edge (similar to the figure in Guo et al. [28])

It can be assumed that the work done by chip formation forces to the material that flows downwards is one source of the stored energy in machined surface layer. And the effective cutting power on machined surface can be expressed as Eq. (2):

$$P_E = P_F + \frac{a}{t}P_C \approx P_F + \frac{r_\varepsilon}{2t}P_C \tag{2}$$

2.2 Energy criterion of stress distribution

It has long been recognized that the cold work done on a specimen may be transformed into heat and stored energy, and the partition of cold work into heat and stored energy depends on the deformation process [29]. Actually, the residual stress field is an important source of stored energy. The material with tensile or compressive residual stress stores energy like the spring being stretched or compressed.

Cutting process itself is a typical large strain, high strain rate plastic deformation process, but for the object in this study, the machined surface and subsurface layer, the plastic strain is far smaller than that in the shear deformation zone where severe shear deformation happens. Figure 3 shows the plastic strain simulation results in face milling of SCM440H, performed with the professional metal cutting simulation and optimization software, Third Wave Systems AdvantEdge. The cutting parameters are as follows: cutting speed is 100.53 m/min, feed per tooth is 0.2 mm, and depth of cut is 0.4 mm. And the Power Law material model of SCM440H and the other FEM settings were the same with Liu et al. [30], which has been proved of acceptable accuracy.

For the residual stress field, the material is in elastic deformation state. As the plastic strain in machined surface is small, to simplify the problem, the following theoretical analysis does not take into account the plastic deformation history during machining process, and the deformation is assumed to be within linear elastic range. In addition, the commonly used metal material can be regarded as isotropic material. Based on the basic laws of elastic mechanics, the strain energy density of one certain point in the residual stress field can be expressed as follows:

$$\begin{aligned} W_R &= \frac{1}{2}\boldsymbol{\sigma} : \boldsymbol{\varepsilon} = \frac{1}{2}\sigma_{ij}\varepsilon_{ij} = \frac{1}{2E}\sigma_{ij}\left[(1+\nu)\sigma_{ij} - \nu\sigma_{kk}\delta_{ij}\right] \\ &= \frac{E}{2(1+\nu)}\left[\frac{\nu}{1-2\nu}\varepsilon_{kk}\delta_{ij} + \varepsilon_{ij}\right]\varepsilon_{ij} \end{aligned} \tag{3}$$

where W_R is the strain energy density; $\boldsymbol{\sigma}$ is the stress tensor, and σ_{ij} $(i, j=1,2,3)$ means the components of stress tensor in three-dimensional space; $\boldsymbol{\varepsilon}$ is the strain tensor, and ε_{ij} $(i, j=1,2,3)$ means the components of strain tensor in three-dimensional space; δ_{ij} is Kronecker δ, whose value is 1 (when $i=j$) or 0 (when $i \neq j$); E is the Young's modulus of the material; ν is the Poisson ratio of the material.

With Eq. (3), one can calculate the strain energy of the residual stress field with residual stress tensor (or the strain tensor). But with currently available measuring techniques, it is difficult to identify all the components of strain or stress tensor in machined surface. For the commonly used X-ray diffraction method, which can only detect the surface residual stresses in most engineering materials, the practical technique is as follows: (a) measure the stresses in two perpendicular directions on surface, (b) remove a thin layer of material with electro-polishing, (c) measure the stresses on new surface, and (d) repeat steps b and c until the stress distribution tend to be stable. Thus, a simplified expression is proposed to estimate the strain energy density with easily accessible components of stress tensor, shown as Eq. (4).

$$W_R = \frac{1}{2}\sigma_{RR}\cdot\varepsilon_{RR} = \frac{1}{2E}\sigma_{RR}^2(z) \tag{4}$$

where σ_{RR} is the resultant stress of the measured two stress components in two perpendicular directions (σ_{Rx} and σ_{Ry}), and $\sigma_{RR} = \sqrt{\sigma_{Rx}^2 + \sigma_{Ry}^2}$; ε_{RR} is the residual strain corresponding to σ_{RR}.

The distribution of residual stresses can be assumed to be uniform for the surface machined with the same parameter within planes parallel to the machined surface, so the strain energy density is a function of the depth from machined

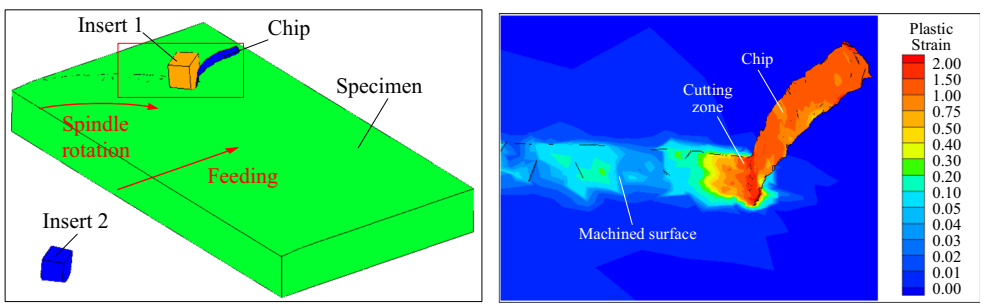

(a) FEM simulation setup (b) Simulated plastic strain after milling

Fig. 3 Estimation of plastic strain on the machined surface with FEM simulation. **a** FEM simulation setup. **b** Simulated plastic strain after milling

Table 1 Chemical composition of SCM440H (% in weight)

C	Si	Mn	P	S	Cr	Mo	Ni	Cu
0.41	0.25	0.77	0.021	0.018	1.09	0.16	0.08	0.09

surface (z). The integral of the strain energy density over depth, which can reflect the quantity of stored energy within the machined surface and subsurface layer caused by machining process, is the first energy criterion and can be calculated with Eq. (5):

$$W_{\mathrm{RI}} = \int_0^{z_s} W_{\mathrm{R}}(z)\cdot \mathrm{d}z \tag{5}$$

where W_{RI} is the integral of the strain energy density over depth, whose dimension is (m/t^2), and the unit in SI (kg-m-s) unit system is (N/m); z_s is the influencing depth of machining-induced residual stresses.

The second energy criterion is defined as the power of stored strain energy, which means the strain energy stored into the workpiece material in unit time during the machining process. And it can be calculated with Eq. (6):

$$P_{\mathrm{R}} = W_{\mathrm{RI}}\cdot v_{\mathrm{c}}\cdot b \tag{6}$$

where P_{R} is the power of stored strain energy, whose dimension is ($m\ L^2/t^3$), and the unit in SI (kg-m-s) unit system is Watt; v_{c} is the cutting speed; b is the uncut chip thickness, i.e., the instantaneous width of cut.

The fraction of the partition of cutting work stored as strain energy (α), as a function of effective cutting power, can be calculated with Eq. (7):

$$\alpha(P_{\mathrm{E}}) = P_{\mathrm{R}}/P_{\mathrm{E}} \tag{7}$$

For the two energy criteria mentioned above, P_{R} is to measure the accumulation rate of energy stored as strain energy during the cutting process, reflecting the properties of the machining process, and W_{RI} is to measure the overall stress state of the machined surface and subsurface layer, which is the final outcome of a certain cutting process.

3 Experiment procedures

To show the validity of the energy criteria, face milling experiments were carried out. The workpiece material used was SCM440H, a low-alloy steel in Japanese Industrial Standard, and its chemical composition is listed in Table 1.

Nine specimens, whose dimensions are 80 mm×30 mm×6 mm, were prepared with SCM440H. The top surfaces of all workpieces were ground with same parameters, and before machining, annealing process with argon gas protection was performed to remove initial stresses. The milling experiment was performed on a DMG machining center, DMU 60 monoBLOCK. The specimen was fixed onto a specially designed fixture with melt adhesive and then the fixture was bolted to a Kistler 9257B dynamometer, as shown in Fig. 4, and the sampling rate of cutting forces was set as 5000 Hz. The cutting forces signal from the dynamometer was amplified by Kistler 5070A Amplifier and then processed with data processing software, Dynoware and Matlab. A 32-mm diameter, two-teeth milling tool was chosen, and carbide inserts were used. The radial and axial rake angles of the milling tool were 2.5° and 5°, respectively; the lead angle was 0°, and the cutting edge radius was 0.04 mm.

To limit the number of tests while fully covering the influence of cutting parameters like cutting speed, feed per tooth, and depth of cut on machining-induced residual stresses. A three-factor and three-level orthogonal experiment design was utilized. The cutting parameters of each test are listed in Table 2. Dry cutting conditions were kept in all experiments.

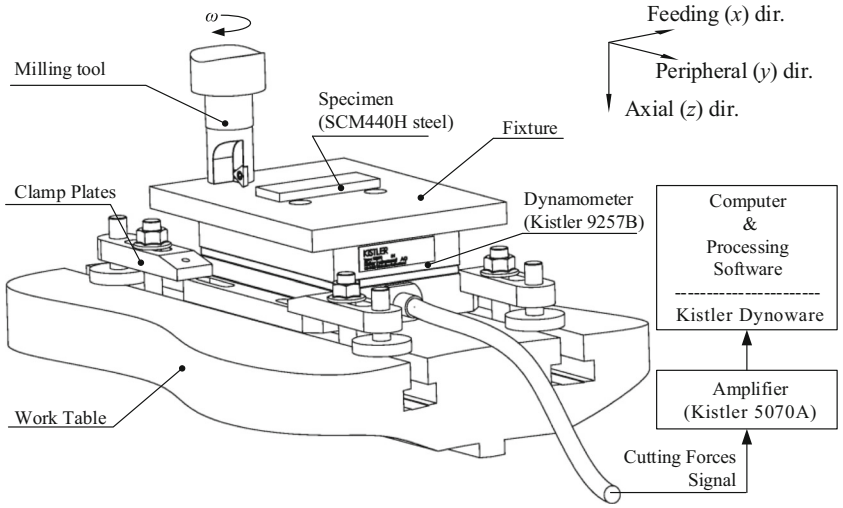

Fig. 4 Setup for milling process and cutting forces measurement

Table 2 Combinations of cutting parameters

Test no.	Spindle speed [rpm]	Feed per tooth [mm]	Depth of cut [mm]
1	1000	0.10	0.2
2	1000	0.15	0.3
3	1000	0.20	0.4
4	1400	0.10	0.3
5	1400	0.15	0.4
6	1400	0.20	0.2
7	1600	0.10	0.4
8	1600	0.15	0.2
9	1600	0.20	0.3

After milling process, the residual stresses were measured with X-350A X-ray diffraction stress analyzer, produced by Handan Stress Technologies Co., Ltd. CrKα tube (20 kV, 5 mA) and 2-mm diameter collimator were used (211), crystal plane was chosen, and the 2θ scanning range was set as 152° to 161°. In order to determine the residual stresses in the sub-surface layer, the electro-polishing technique was used. The in-depth distribution residual stresses along x (feeding) and y (peripheral) directions (σ_{Rx} and σ_{Ry}, respectively) were measured at the central point of the workpiece, as shown in Fig. 5.

4 Results and discussion

4.1 Analysis of cutting forces

The cutting forces changed periodically during the milling process. Figure 6 shows the original measured data for test no. 1 within one cutting cycle. As the residual stresses at the central point of the specimens were studied, the cutting forces at central line was calculated by averaging the 20 points of the originally measured data near the central line in each cutting cycle and then averaging these central values of all the stable cutting cycles. The results are shown in Fig. 7, where F_{xC}, F_{yC}, and F_{zC} are the cutting forces along feeding, peripheral, and axial directions at the central line, which are the same with radial, tangential, and axial directions in the tool coordinate system, respectively.

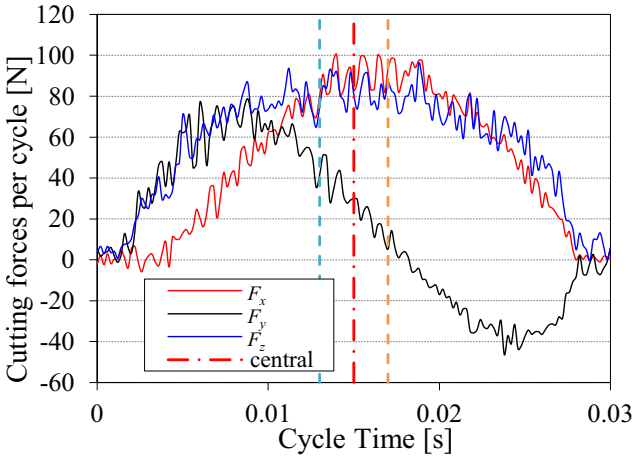

Fig. 6 Original measured data of the three-directional cutting forces

4.2 Measured residual stress distribution

After machining, the in-depth distribution of residual stresses along feeding and peripheral directions was measured, and the resultant residual stress was calculated, as shown in Fig. 8. The residual stresses along the two directions change approximately simultaneously for each test. The machining-induced residual stresses in feeding and peripheral directions are both tensile at the machined surface and fall off to a maximum compressive state with the increase in depth, after which the compressive stresses decrease and approach a steady value next to zero in near workpiece substrate. The energy criterion, P_R and W_{RI}, were calculated with Eqs. (4)–(6).

4.3 The influence of effective cutting power

A key factor for the calculation of cutting power with measured cutting forces is the friction coefficient (μ) between SCM440H (workpiece material) and cemented carbide (tool material). Lan et al. [31] carried out experiments on the machining of SCM440H with cemented carbide inserts, and the results indicated that μ is dependent on the cutting parameters, or more exactly, the consequent temperature, the normal stress, and the speed of relative movement. Further research on building an accurate model still needs to be carried out, yet

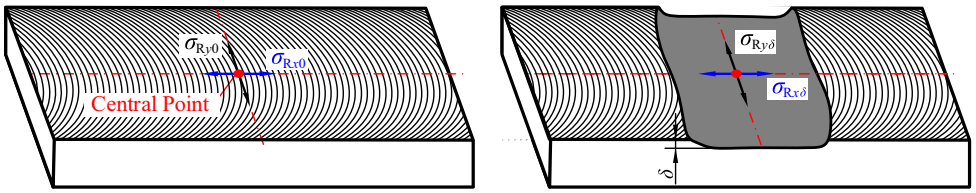

Fig. 5 Measurement of the in-depth distribution of residual stresses. **a** Measurement of surface stresses. **b** Measurement of subsurface stresses

(a) Measurement of surface stresses (b) Measurement of sub-surface stresses

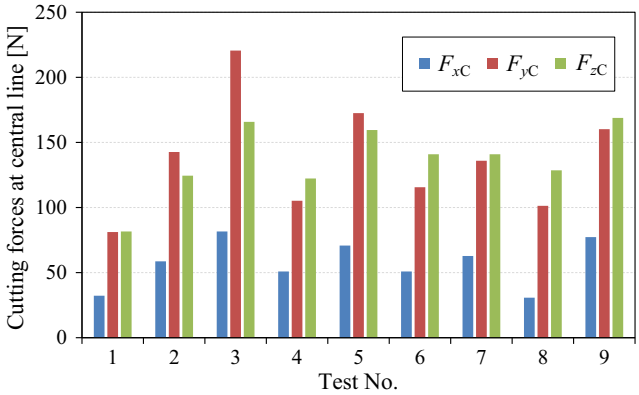

Fig. 7 Three-directional cutting forces at central line

for a simplified qualitative analysis, in this study, μ was set as a constant 0.65.

The Young's modulus of SCM440H is 2.1×10^{11} Pa. And at the central line, the speed of tool tip in feeding direction (v_x) is equal to the feeding speed (v_f), and the speed of tool tip in peripheral direction (v_y) is equal to the main cutting speed (v_c):

$$\begin{aligned} v_x &= v_f = Nf_z n \\ v_y &= v_c = \pi D n \end{aligned} \tag{8}$$

where N is the number of teeth (=2); f_z is feed per tooth; n is the spindle speed; D is the diameter of tool (=32 mm).

With the data in Table 2 and Fig. 7, and Eqs. (1) and (2), the items concerning the effective cutting power were calculated. The influence of effective cutting power on the value of surface residual stresses and the variables about the stored strain energy were analyzed, as shown in Fig. 9.

According to Fig. 9a, with the increase of the effective cutting power, the tensile residual stresses on the machined surface tend to become larger. According to the commonly accepted formation mechanism of machining-induced residual stresses [3, 32], the stress curves shown in Fig. 8 indicate that the thermal loads and frictional loads play the main role in deciding the stress distribution pattern under the experimental

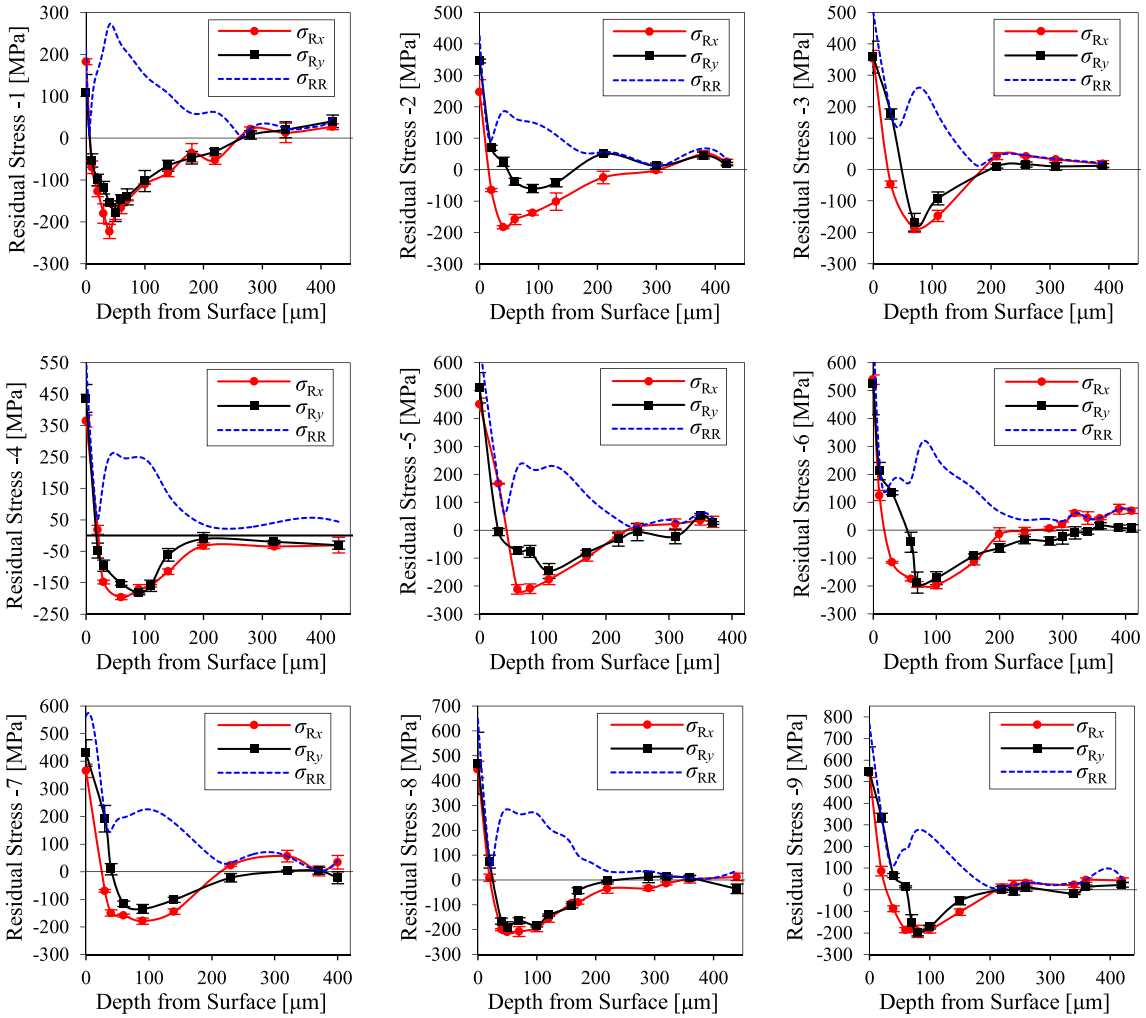

Fig. 8 In-depth distribution of machining-induced residual stresses

conditions of this study. And these loads are all in positive correlation with the effective cutting power calculated with Eq. (2).

Figure 9b, c indicates that under the designed experimental conditions, the power of strain energy increases at growing rate with the increase of effective cutting power. The discrete data in Fig. 9b can be fitted with a second-order polynomial, as Eq. (9), and correlation coefficient R^2=0.849.

$$P_R = 0.0002P_E^2 - 0.07P_E \tag{9}$$

where P_R and P_E are in Watt.

The experimental research of Hodowany et al. [33] shows that for the representative rate-insensitive and rate-sensitive materials and under different strain rates, with the increase of cold work and the consequent plastic strain, the fraction of the rate of cold work dissipated as heat (β) firstly decreases, then reaches a relatively steady state, and later becomes larger with the further increase of plastic strain. In normal machining, the temperature is not very high and it can be assumed that no phase change and chemical reaction happen in this process. Thus, it can be further assumed that the cold work done during machining process either dissipates as heat or be stored in the residual stress field, i.e., $\alpha+\beta=1$. As analyzed, the plastic strain in the machined surface layer is not very big, and thus, in normal cutting process, α for the machined surface may lie in the range where it increases with the increase of effective cutting power, which may qualitatively explain the curves in Fig. 9b, c. And a specific research into the partition of cold work into heat and stored energy for SCM440H material under cutting conditions will be carried out in the future.

Figure 9d shows that the stored strain energy within the machined surface and subsurface layer is approximately in direct proportion to the effective cutting power. The calculated data can be fitted with Eq. (10) with a fine correlation coefficient R^2=0.917. The cutting power is in positive relation with cutting speeds. With larger speeds, the cutting power grow larger, but the time to machine unit volume of material and to generate the corresponding unit area of machined surface become smaller, which achieves a delicate balance to form the linear relation. The proposed criterion W_{RI} might be useful in predicting the stress distribution.

$$W_{RI} = 0.1094P_E \tag{10}$$

where W_{RI} is in newton per meter, and P_E is in Watt.

5 Summary

In this paper, a new approach to evaluate, analyze, and predict the machining-induced residual stresses was proposed. The cutting parameters, the cutting loads, and the evaluation of residual stress field are unified to the concept of energy. The effective cutting power on the machined surface was analyzed, and the integral of strain energy density over depth

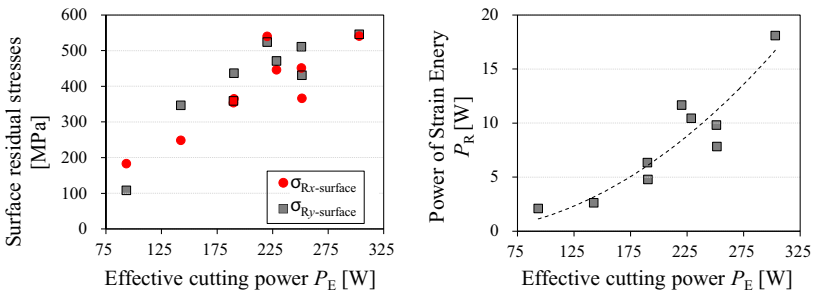

(a) Influence on surface stresses

(b) Influence on power of stored energy

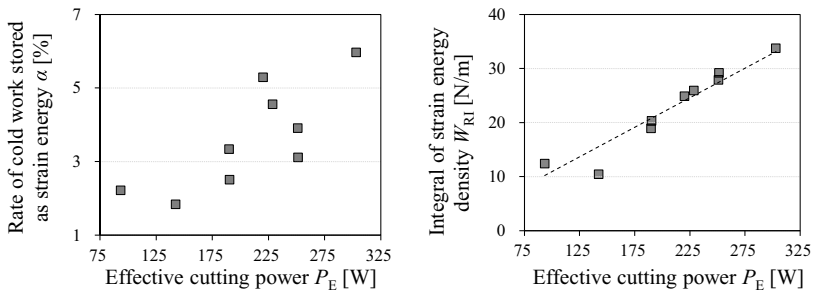

(c) Influence on rate of cold work stored as strain energy

(d) Influence on integral of strain energy density over depth

Fig. 9 The influence of effective power on residual stress distribution. **a** Influence on surface stresses. **b** Influence on power of stored energy. **c** Influence on rate of cold work stored as strain energy. **d** Influence on integral of strain energy density over depth

and power of stored strain energy were supposed to be the energy criteria of machining-induced residual stresses. With the theoretical analysis and the experimental results in this paper, the following conclusions can be drawn:

(1) The residual stress field is a strain energy field. The overall distribution state of residual stresses, including the value and existing range, is correlated to the amount of energy stored. Thus, the proposed energy criterion, the integral of strain energy density over depth and the power of stored strain energy, can be used to evaluate the stress distribution.
(2) Under the experimental conditions of this study and many other machining experiments, the surface residual stresses are tensile, which indicates that the frictional force and thermal effects play the main role in deciding the final stress distribution.
(3) For normal machining process (or at least the conditions in this study), as the plastic strain of the machined surface is small, the fraction of partition of mechanical work stored as strain energy tends to be larger with the increase of effective cutting power. And the consequence of this trend is that the power of stored strain energy increases at growing rate with the increase of effective cutting power.
(4) With the increase of effective cutting power, and to some extent the corresponding decrease of time consumption to generate unit area of machined surface, the integral of strain energy density over depth, which measures the amount of energy, increases approximately linearly in this study.

The analysis of energy criteria and cutting power may provide a new approach to analyze and model the machining-induced residual stress, as they can reflect the relation among cutting parameters, cutting loads, and stress field. And more successive research will be carried out to confirm the feasibility of the method.

Acknowledgments This research is supported by the Key National Science and Technology Projects of China (Grant No. 2013ZX04001-011) and Beijing Municipal Natural Science Foundation (Grant No. 3141001).

References

1. Sasahara H (2005) The effect on fatigue life of residual stress and surface hardness resulting from different cutting conditions of 0.45 % C steel. Int J Mach Tools Manuf 45(2):131–136. doi:10.1016/j.ijmachtools.2004.08.002
2. Wan Y, Cheng K, Fu XL, Liu ZQ (2013) An experiment-based investigation on surface corrosion resistance behaviors of aluminum alloy 7050-T7451 after end milling. Proc Inst Mech Eng J J Eng Tribol 227(11):1297–1305. doi:10.1177/1350650113491084
3. Schajer GS, Ruud CO (2013) Overview of residual stresses and their measurement. In: Schajer GS (ed) Practical residual stress measurement methods. John Wiley & Sons, pp 1–27
4. Masoudi S, Amini S, Saeidi E, Eslami-Chalander H (2015) Effect of machining-induced residual stress on the distortion of thin-walled parts. Int J Adv Manuf Technol 76(1-4):597–608. doi:10.1007/s00170-014-6281-x
5. Outeiro JC, Dias AM, Lebrun JL, Astakhov VP (2002) Machining residual stresses in AISI 316L steel and their correlation with the cutting parameters. Mach Sci Technol 6(2):251–270. doi:10.1081/MST-120005959
6. El-Khabeery MM, Fattouh M (1989) Residual stress distribution caused by milling. Int J Mach Tools Manuf 29(3):391–401. doi:10.1016/0890-6955(89)90008-4
7. El-Axir MH (2002) A method of modeling residual stress distribution in turning for different materials. Int J Mach Tools Manuf 42(9):1055–1063. doi:10.1016/S0890-6955(02)00031-7
8. Capello E (2005) Residual stresses in turning: part I: influence of process parameters. J Mater Process Technol 160(2):221–228. doi:10.1016/j.jmatprotec.2004.06.012
9. Capello E (2006) Residual stresses in turning: part II. Influence of the machined material. J Mater Process Technol 172(3):319–326. doi:10.1016/j.jmatprotec.2005.10.009
10. He AD, Ye BY, Qin MY (2012) Influence of machining parameters and pre-stress on residual stress of pre-stress hard turning in 40 Cr steel. Appl Mech Mater 157–158:400–405. doi:10.4028/www.scientific.net/AMM.157-158.400
11. Jafarian F, Amirabadi H, Fattahi M (2014) Improving surface integrity in finish machining of Inconel 718 alloy using intelligent systems. Int J Adv Manuf Technol 71(5-8):817–827. doi:10.1007/s00170-013-5528-2
12. M'Saoubi R, Outeiro JC, Changeux B, Lebrun JL, Mor O, Dias A (1999) Residual stress analysis in orthogonal machining of standard and resulfurized AISI 316L steels. J Mater Process Technol 96(1):225–233. doi:10.1016/S0924-0136(99)00359-3
13. Arunachalam RM, Mannan MA, Spowage AC (2004) Residual stress and surface roughness when facing age hardened Inconel 718 with CBN and ceramic cutting tools. Int J Mach Tools Manuf 44(9):879–887. doi:10.1016/j.ijmachtools.2004.02.016
14. Zong WJ, Li D, Cheng K, Sun T, Liang YC (2007) Finite element optimization of diamond tool geometry and cutting-process parameters based on surface residual stresses. Int J Adv Manuf Technol 32(7-8):666–674. doi:10.1007/s00170-005-0388-z
15. Withers PJ, Bhadeshia HKDH (2001) Residual stress. Part 2—nature and origins. Mater Sci Technol 17(4):366–375. doi:10.1179/026708301101510087
16. Su JC, Young KA, Ma K, Srivatsa S, Morehouse JB, Liang SY (2013) Modeling of residual stresses in milling. Int J Adv Manuf Technol 65(5-8):717–733. doi:10.1007/s00170-012-4211-3
17. Ji X, Zhang XP, Liang SY (2014) Predictive modeling of residual stress in minimum quantity lubrication machining. Int J Adv Manuf Technol 70(9-12):2159–2168. doi:10.1007/s00170-013-5439-2
18. Yao CF, Wu DX, Tan L, Ren JX, Shi KN, Yang ZC (2013) Effects of cutting parameters on surface residual stress and its mechanism in high-speed milling of TB6. Proc Inst Mech Eng B J Eng Manuf 227(4):483–493. doi:10.1177/0954405413475771
19. Ma Y, Yu DW, Feng PF (2014) FEM analysis of residual stress distribution and cutting forces in orthogonal cutting with different initial stresses. Mater Sci Forum 800–801:380–384. doi:10.4028/www.scientific.net/MSF.800-801.380
20. Özel T, Ulutan D (2012) Prediction of machining induced residual stresses in turning of titanium and nickel based alloys with experiments and finite element simulations. CIRP Ann Manuf Technol 61(1):547–550. doi:10.1016/j.cirp.2012.03.100
21. Liu M, Takagi J, Tsukuda A (2004) Effect of tool nose radius and tool wear on residual stress distribution in hard turning of bearing

steel. J Mater Process Technol 150(3):234–241. doi:10.1016/j.jmatprotec.2004.02.038
22. Jiang XH, Li BZ, Yang JG, Zuo X (2013) Effects of tool diameters on the residual stress and distortion induced by milling of thin-walled part. Int J Adv Manuf Technol 68(1-4):175–186. doi:10.1007/s00170-012-4717-8
23. Yeung H, Sundaram NK, Mann JB, Dale Compton W, Chandrasekar S (2013) Energy dissipation in modulation assisted machining. Int J Mach Tools Manuf 74:41–49. doi:10.1016/j.ijmachtools.2013.07.007
24. Akyildiz HK, Livatyali H (2014) Effect of cutting energy on fatigue behavior of threaded specimens. Int J Adv Manuf Technol 70(1-4):547–557. doi:10.1007/s00170-013-5278-1
25. Shao H, Wang HL, Zhao XM (2004) A cutting power model for tool wear monitoring in milling. Int J Mach Tools Manuf 44(14):1503–1509. doi:10.1016/j.ijmachtools.2004.05.003
26. Fang N (2005) Tool-chip friction in machining with a large negative rake angle tool. Wear 258(5-6):890–897. doi:10.1016/j.wear.2004.09.047
27. Ozturk S, Altan E (2013) Position of the separation point in machining with a rounded-edge tool. Proc Inst Mech Eng B J Eng Manuf 227(7):965–971. doi:10.1177/0954405413484137
28. Guo YB, Anurag S, Jawahir IS (2009) A novel hybrid predictive model and validation of unique hook-shaped residual stress profiles in hard turning. CIRP Ann Manuf Technol 58(1):81–84. doi:10.1016/j.cirp.2009.03.110
29. Taylor GI, Quinney H (1934) The latent energy remaining in a metal after cold working. Proc R Soc London Ser A, Containing Pap Math Phys Charact 143(A849):307–326. doi:10.1098/rspa.1934.0004
30. Liu S, Zhang JF, Feng PF, Yu DW, Wu ZJ (2012) Determination of constitutive equation parameters for face milling 3-D simulation via pressure bar and orthogonal cutting tests. Mater Sci Forum 723:136–142. doi:10.4028/www.scientific.net/MSF.723.136
31. Lan B, Feng PF, Wu ZJ, Yu DW (2012) Determination of constitutive equation parameters for orthogonal cutting through pressure bar tests and FEA method. Key Eng Mater 499:56–61. doi:10.4028/www.scientific.net/KEM.499.56
32. Wu DW, Matsumoto Y (1990) The effect of hardness on residual stresses in orthogonal machining of AISI 4340 steel. J Manuf Sci Eng Trans ASME 112(3):245–252. doi:10.1115/1.2899582
33. Hodowany J, Ravichandran G, Rosakis AJ, Rosakis P (2000) Partition of plastic work into heat and stored energy in metals. Exp Mech 40(2):113–123. doi:10.1007/BF02325036